Journal of Geomine (2024), 2(2), 69-77 DOI: 10.22077/jgm.2025.8381.1040



Petrology and temperature determination of skarn formation in Dezg area, southwestern of Hajiabad, north of Birjand

Gholamreza Fotoohi Rad¹, Mohammad Hossein Yousefzadeh², Zohreh Esmaeili³

Recived: 2024 Nov. 05, Revised: 2025 Feb. 08, Accepted: 2025 Apr. 05, Published: 2025 Apr. 12



Journal of Geomine © 2024 by University of Birjand is licensed under CC BY 4.0

ABSTRACT

The study area is located north of Dezq village in southwestern of Hagiabad. Mineralogical and geochemical investigations are showing two main stages of prograde and retrograde metamorphism in formation of skarn in study area. In prograde stage, has formed skarn with anhydrous silicate- calcium mineral assemblage (andradite – grossular and diopside-hedenbergite) in temperature range of 328° to 599° which has similar composition with garnets from Cu- Fe and Au skarns. Formation of anhydrous calcium silicate minerals like andradite, grossular, and clinopyroxene proves the temperature range between 756 and 776°C and XCO2=0.1-0.6. In retrograde stage,a part of these anhydrous silicates at temperatures lower than 756°C are affected by retrograde metamorphism and changed to hydrous and anhydrous silicate minerals with less calcium(epidote, tremolite-actinolite) and finally hydrous and anhydrous calcium assemblage has altered to fine grain minerals including chlorite, calcite, quartz and clay minerals in temperature range of less than 300°. The presence of intergrowth texture and absence of replacement texture in andradite and pyroxene, is showing that these minerals are formed as contemporaneous. This mineral assembelage has crystallized in high partial water pressure which is between 0.8 to 0.9 whole pressure. High partial water pressure has been certainly result of water fluid seepage from granitic body to country rock.

KEYWORDS

Garnet, prograde metamorphism, retrograde metamorphism, Sistan suture, skarn

I. INTRODUCTION

The study area (near the village of Dezg) is a part of Sistan suture zone in the East (Eastern Mountains) of Iran extending from northwest to southeast and located near the village of Surand. Dezg is located in the southwest of Hajiabad within the longitudes of $60^{\circ}06'57.47''$ to $60^{\circ}04'11.11''$ east and latitudes of 33º20'25.27" to 33º22'02.93" north on Shahrokht map 1:250000 (Alavi Naeeini, 1981) and Ahangaran map 1:100000 (Alavi Naeeini, 1982). In most tectonicsedimentary classifications, this part of Iran has been introduced as the Sistan structural zone. Sistan suture zone is another name that researchers have used for this area (Tirrul et al., 1983). Located in the east vicinity of the study area, the region's highlands are made of lime stones as old as Lower Cretaceous and Paleocene (Fotoohi Rad, 2004, 2005; Angiboust et al., 2013; Bröcker et al., 2013]. In the south of the region, an assemblage of tonalite igneous rocks and granodiorite can be seen, and the west is covered with igneous rocks belonging to ophiolite complex that are mostly peridotites. Among the metamorphic rocks observed in the region are granulite, amphibolite, epidote amphibolite, green schist, and skarn (Esmaeili, 2014).

The present investigation's main aim was the study of mineral chemistry and temperature of skarn formation. Because of Skarns are very important ore deposits and usually are economically important deposits, this study was necessary in study area to specify formation conditions of Skarn of study area.

II. GEOLOGY OF THE AREA

As mention in Introduction, the study area is a part of Sistan suture zone in the East of Iran that extends from northwest to southeast on Shahrakht map 1:250000 (Alavi Naeeini, 1981) (See Fig. 1). In fact, the study region is an ophiolite complex that is an almost complete sequence of ultramafic to mafic igneous rocks (partially metamorphosed) and radiolarian cherts and radiolarites (partially metamorphosed) and has a specific metamorphic zone in the eastern part. The above rock complex is interdigital located with one another and to other components of the ophiolitic complex.

Ophiolitic sequence is not well observable due to bearing of different tectonic activities. In some points of the region, however, almost no specific sequence can be seen. In these points, metamorphic zone rocks to ultramafic rocks, gabbro, very specific metamorphosed sheet dikes, basalt to andesite basalt, and specific bedding can be observed in gabbroic rocks.

¹ Department of Mining Engineering, Faculty of Engineering, University of Birjand, Birjand, Iran, ² Department of Geology, University of Birjand, Birjand, Iran, ³ MSc. of Petrology, Department of Geology, University of Birjand, Birjand, Iran

☑ Gh. Fotoohi Rad: gfotohirad@birjand.ac.ir



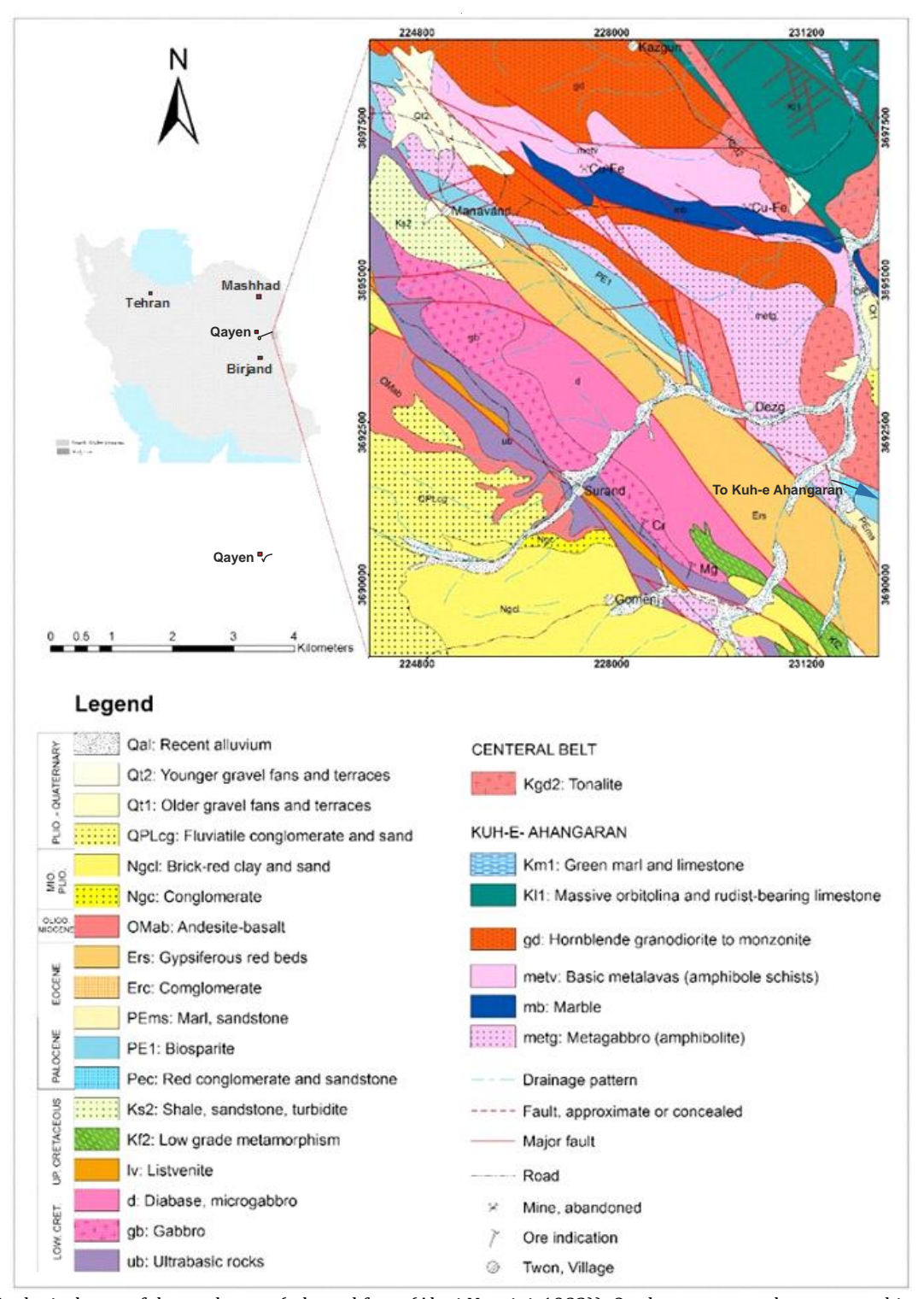


Fig. 1. Geological map of the study area (adapted from (Alavi Naeeini, 1982)). On the map metg show greenschist, epidote amphibolite and some granulite facies rocks. The granulite is more in next to Dezg village

In the south of the region, there are an assemblage of tonalite and granodiorite igneous rocks, and formation of skarn can be as a result of adjacency of this intrusive bodies with rocks containing skarn in further depth, and the formed skarn comes to the surface of the ground. Mineralogical examination is an important tool in identifying and determining the type of the skarns. Moreover, mineralogy is an important factor in figuring out the origin of the skarns, the formation temperature,

and the identification of minerals with economic value. Due to its combination with other suitable minerals, garnet acts as a good geothermobarometr. In general, calcic skarns form from metasomatism of limestones in the final stages of replacement of an intrusion at shallow depths. Main minerals of calcic skarns are including garnet (Grossular - Andradite), clinopyroxene (diopside - hedenbergite), epidote, vesuvianite, scapolite, wollastonite, magnetite, etc. which are identifiable



depending on the transformation degree and the effects of processes of retrograde metamorphism on the aureole formed at the metamorphic peak in different zones. Petrographic studies and also fluid inclusion studies play an important role in understanding skarn formation process and the path taken in pressure-temperature diagram.

III. METHODS

In the present study, a reference (Esmaeili, 2014) was used to collect the required data. After relevant reports, maps, and studies were examined, field observations were made several times in order to examine the border of rock units, collect samples, and take photos.

Afterwards, among the 176 collected sample rocks (Esmaeili, 2014); 116 samples with thin section and 16 with polished section were prepared and examined with polarizing microscope and reflected light. In these examination, different mineral collections identified in metamorphic rocks in order to determine metamorphic facies, and examination transformations of these rocks was carried out based on conversion of minerals into one another and finally by determining different stages of metamorphism and its intensity and extent in the region (Esmaeili, 2014). Five skarn samples were selected for chemical analysis by the XRF method (See Table 1). Moreover, microprobe analysis was carried out on five rock samples with the maximum degree of metamorphism including minerals garnet, clinopyroxenes, feldspar, and amphibole in University of Münster, Germany to determine formation pressure and temperature of skarn. The results are presented in Tables 2 and 3.

Table 1. Results of XRF analysis, 5 samples of the metamorphic rocks of the area

metamorphic rocks of the area								
Oxides/Sample	35	18	28	23	26			
SiO ₂	50.8	52.5	53	46.7	50.3			
Al ₂ O ₃	14.3	13.6	6.3	15.3	11.1			
Fe ₂ O ₃	10.3	12.4	10.9	12.8	10.6			
Mg0	5.9	4.7	13.5	4.7	10.5			
CaO	12.3	11.6	12.5	14.6	13			
SO ₃	0.1	0.1	< 0.1	0.1	0.2			
K ₂ O	0.3	0.1	< 0.1	0.2	0.1			
Na ₂ O	2.9	3	0.4	1.3	0.9			
TiO2	1	0.7	0.4	0.7	0.7			
MnO	0.2	0.1	0.2	0.2	0.3			
$P_{2}O_{5}$	0.2	0.1	< 0.1	0.1	0.1			
Cr ₂ O ₃	< 0.1	< 0.1	0.2	< 0.1	0.2			
NiO	< 0.1	< 0.1	0.1	-	< 0.1			
L.O.I	1.35	0.61	2.04	0.94	1.54			
Total	99.85	99.71	99.84	99.44	99.66			

IV. GEOLOGY AND PETROGRAPHY OF SKARN

In the study area, there are skarns whose main minerals are epidotic, grassular, andradite, diopside, and calcite and less quartz, sphene, and hornblende. These skarns have generally developed inside calc-silicate rock fractures or on the border of limestone, marl, pelitic and semi-pelitic rocks.

Formation of such skarns is possible in different metamorphic regions (Kretz, 1994). Formation of these skarns are the result of local metasomatic reactions that happen during regional metamorphism. In this type of skarns like all other skarns; therefore, fluids need to be active in the environment. Intrusive igneous bodies are the source of these fluids in common skarns (Daya and Hosseini-Nasab, 2017; 2019; Daya et al., 2024). During prograde metamorphism, decarbonization dehydration reactions occur, and amounts of CO2 and H₂O are produced, which move toward the weak points of rocks (Meinert, 2013). These weak points which fluids can flow through and concentrate at are lithologic boundaries (Cartwright, 1994; Jamteveit et al., 1992). Cracks in rocks are also a suitable environment are also environments for the movement concentration of these fluids (Meinert, 2013). The fluids mostly dissolve some components of the primary rock and transfer them to the host rock. The fluids derived from limestones are usually full in CO2 and Ca, while fluids obtained from pelitic rocks may contain some Fe, K, Na, and Si (Meinert, 2013). Entrance of a fluid derived from carbonate rocks to pelitic rocks, or vice versa, results in metasomatism and thus develops skarns. Since chemical potential of CO2 decreases as a result of production of calc-silicate layers and chemical potential of H₂O as a result of production of pelitic rocks in contact between the two layers of pelitic rock and calc-silicate (Zhai et al., 2014), these areas are suitable environments for reactions that lead to formation of skarns. That is why the above skarns develop in lithologic contact of calcsilicate and carbonate rocks with pelitic rocks, or in general, in areas containing layers with incompatible composition. On the other hand, some fluids also migrate into cracks and fractures of surrounding rocks, react with host rocks, and form skarns that are limited to fractures. In the Workshop of Skarn Deposits (Meinert, 2013), a model for formation of skarns was proposed, which is presented in Fig. 2 which is in fact a summary of the above discussion on how skarns form.

In Dezg area, skarn has developed inside igneous intrusive bodies or calc-silicate rock fractures. According to the above mentioned information and the model proposed in Workshop of Skarn Deposits (Meinert, 2013) presented in Fig. 2, formation of skarns in the region can be attributed to the function of the igneous intrusive bodies and Contact metamorphism.

In these skarns, large hypidiomorphic pink crystals of garnet can be observed, such that abundance of garnet gives a bright muddy color to the rock. These skarns are well developed in the southeast and east areas of Dezg. Microscopic examinations indicated that the major part of the rock is composed of garnet minerals (See Fig. 3), clinopyroxene, and plagioclase formed in parts with epidote section are also observed, which may be as a result of retrograde metamorphism.



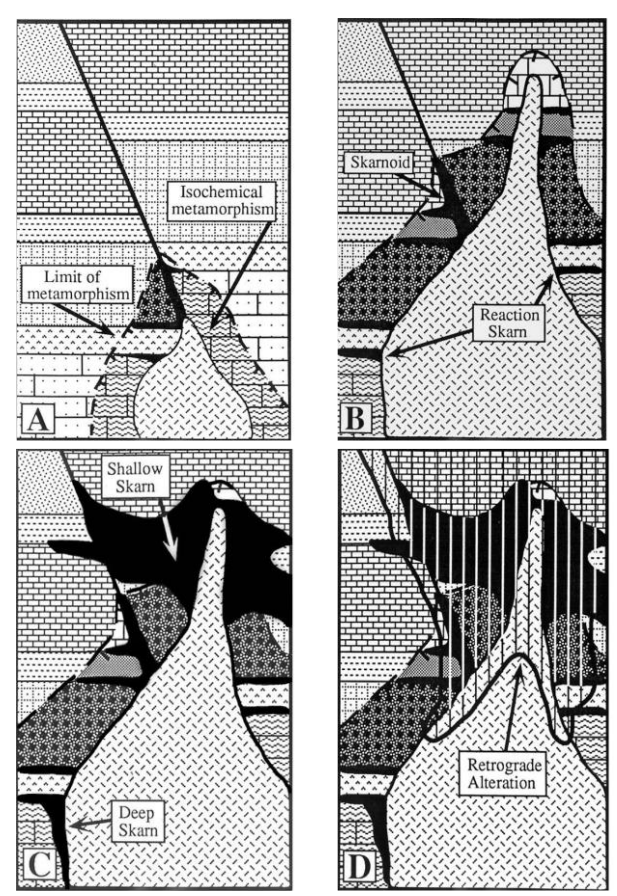


Fig. 2. The model of skarn formation in the study area (Meinert, 2013)

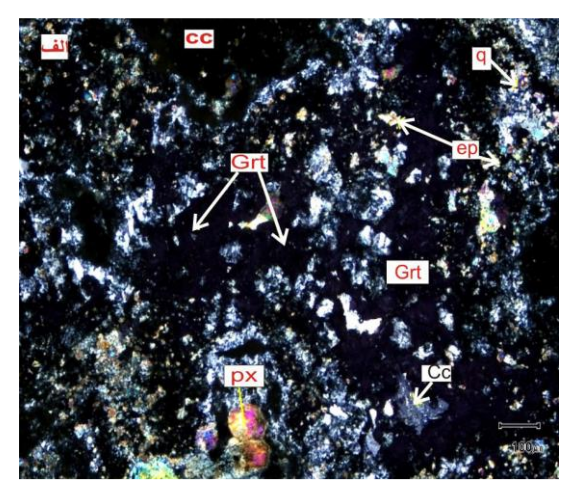


Fig. 3. Skarn garnets in the southwest of Dezg

Garnets belong to ugrandite (andradite – grossular) group and form the main part of shaped and amorphous rocks. Quartz and clay minerals are also present; however, their amount is limited. Almost all of these rocks are affected by the solutions derived from igneous intrusive bodies, which led to contact metamorphism and skarn formation.

Two types of metamorphism stage in skarn system include primary prograde stage which is associated with anhydrous minerals like garnet and pyroxene, and final retrograde stage which is characterized by hydrous minerals including epidote, hornblende, calcite, quartz, and chlorite. In prograde stage, due to deposit of

anhydrous calcium silicate minerals, andradite, grossular, and clinopyroxene, the temperature range between 756 and 776°C and XCO2=0.1-0.6 can be expressed. In the retrograde metamorphism stage at temperatures lower than 756°C, an assemblage of anhydrous calcium silicate minerals has changed into hydrous silicate minerals like epidote minerals. Moreover finally, the assemblage of hydrous and anhydrous calcium silicate minerals undergo metamorphism and turn into fine mineral assemblages like chlorite, calcite, quartz, and clay minerals.

A. Mineral chemistry of metamorphic rocks

In this section, mineral chemistry of metamorphic rocks of the region studied using electron microprobe analysis in University of Münster, Germany are presented. The results of electron microprobe analysis of these minerals are presented in Tables 2 and 3.

B. Garnet

Garnet is one of the main skarn minerals in Dezg. Table 2 presents the results of electron microprobe analysis of garnet in a skarn sample of Dezg. Based on the collected field data, it was concluded that rock units in this region are affected by tectonic activities. Therefore, under the influence of shearing activity of minor faults, cracks and fractures form in limestones. This permeable network is an important factor for leakage of hydrothermal solutions and mineralization of calcium garnets by providing channels for flow of magmatic volatiles or volatiles and products obtained from thermal metamorphic reactions. Fig.s 4 and 5 present the composition of garnets in relevant diagrams. Garnet is from index minerals of skarns in Dezg. Since this mineral forms in the final stages of mineralization, it is almost seen in different Subhedral to Euhedral shapes.

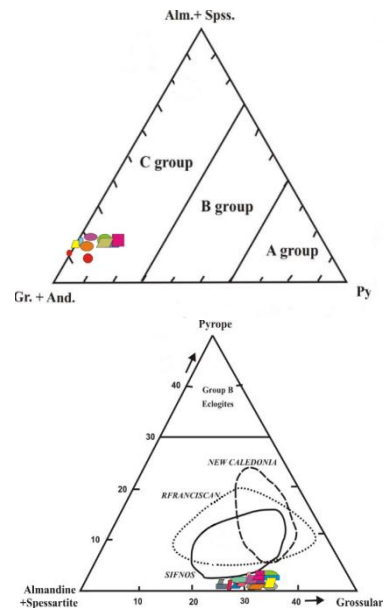


Fig. 4. Index diagram of skarn garnets in the southwest of Dezg (Derived from (Esmaeili, 2014))



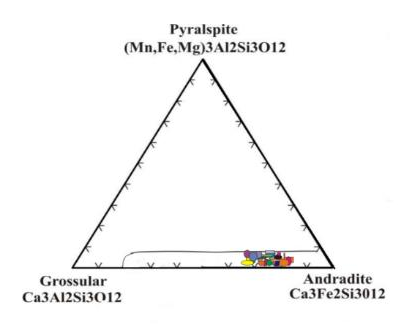


Fig. 5. The position of the garnets in andradite – grossular area (Esmaeili, 2014)

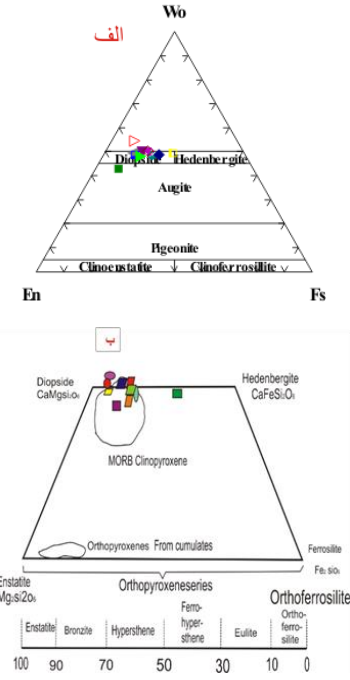


Fig. 6. (a) Variations of clinopyroxene composition skarn samples existing in the southeast of Dezg (Esmaeili, 2014), (b) Quadrilateral chart of pyroxenes, which indicates the presence of diopside and augite diopside in skarn samples (Esmaeili, 2014)

C. Pyroxene (a)

The results of electronic micro-processing analysis of clinopyroxenes of the study area are presented in Table 3. According to Diagram 6, composition of clinopyroxenes is the same and places in the field of diopside to augite diopside and hedenbergite. According to the diagram presented in Fig. 7, all clinopyroxenes have metamorphic nature, which indicates that this mineral has crystalized in metamorphism conditions. The rate of changes i (b) 13 was from 0.16 to 5.61 weight percent (Wt%), and CaO changes from 21.4 to 25.06 Wt%.

D. Geothermobarometry

One of the issues that has nowadays developed in metamorphic rocks is to determine the formation pressure and temperature of rocks (thermobarometry). A method to estimate the formation pressure – temperature of minerals in balance state is to use

individual thermobarometer which is independently regulated based on experimental or thermodynamic data. In order to measure the formation temperature and pressure of mineral assemblages in the present study, thermobarometers with balanced pair minerals or single minerals were employed (Kerog, 1988). Fig. 1 is the simplified geology of the study region and indicates exposure of rock samples on which thermobarometry have carried out.

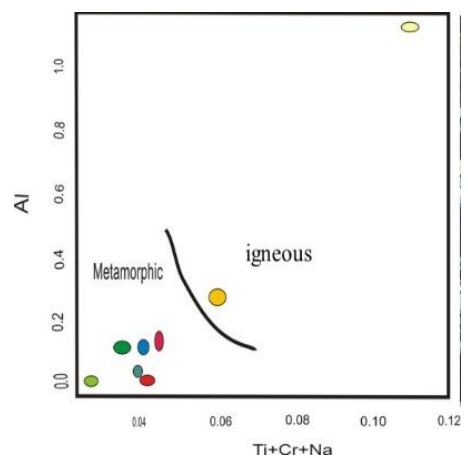


Fig. 7. Diagram Cr + Na + Ti compared to Al indicates that more clinopyroxenes have metamorphic nature

E. Geothermobarometry based on a type of pyroxene

Mercier (1980) proposed thermometers and barometers based on clinopyroxene or orthopyroxene to determine the crystallization temperature and pressure of garnet peridotites and spinel peridotites. These calibrations are based on the effect of Cr on the solubility of Al. Therefore, these thermometers and barometers apply to chromium-rich mineral assemblages (Zhai et al., 2014). These single-pyroxene thermometers and barometers are designed based on thermodynamic principles. The following Eq.s. are valid for clinopyroxenes:

 $T_{CPX}(^{9}C) = [(-7537.5 \text{ AlogX }_{KW} + 61152) / D]-273$ $P_{CPX}(Kb) = [(419.76 \text{ AlogX }_{KW}-706.14 \text{ AlogX }_{KA} + 616.61)]/D$ That:

 $X_{KW} = (1-2W) / (0.667+0.667W)$

 $X_{KA} = A/(1-A)(1-1.27 F_{Cr})^2$

$$\begin{split} & D \! = \! ALogX_{KA}ALogX_{KW} \! + \! 11.2724ALogX_{KW} \! + \! 2.2595ALogX_{KA} \! + \! 32.371 \\ & W = Ca/(Ca(+Mg \! + \! Fe^2 \! + \! Mn), \end{split}$$

A = (Al-Na)/2, $F_{Cr} = Cr/(Al+Cr-Na)$

V. GEOTHERMOBAROMETRY AND DISCUSSION

In the studied metamorphic rocks, according to the balanced minerals in different metamorphic facies and by using the results of microprobe analyses, the activity of end members of mineral can be achieved through "Active.exe" software for end members of each mineral,



then, Ptmafic software is employed to determine formation and crystallization temperature and pressure of mineral assemblages of these rocks (Parkins and Newton, 1981).

A. The results of geothermobarometry in skarn samples

Based on the microprobe data and the relevant software, the obtained temperatures, and pressures are presented in Tables 4, 5, and 6. The range of the conducted reactions and the taken path are indicated on the diagram of Fig. 8. Therefore, V (pyroxene-garnet facies) and VI (pyroxene epidote facies) can be observed in the study area. The consequences of retrograde metamorphism under the influence of hydrothermal, metamorphic, or cooler water fluids full in H_2O result in formation of hydrous minerals like epidote. Conversion of garnet into epidote and pyroxene into actinolite and chlorite can be evidence for occurrence of retrograde metamorphism in evolution of skarn in the region.

According to the diagram presented in Fig. 8, the metamorphism of skarn in the area is of average degree. In Fig. 8, which is the range of the facies in skarn in diagram P-T, the boundary between the facies is indicated using a series of key reactions (Zharikov, 1991).

In general, two facies of hornblende-hornfels and albite epidote-hornfels can be observed.

Hornblende-hornfels facies: This facies formed in a temperature between 420 and 925°C and pressure of 3-5 Kb. Yardley (1981) believes that hornblende-hornfels facie can be named low pressure amphibolite facies. Mineral paragenesis diopside + calcite places in the end of this facies and the beginning of pyroxene-hornfels facies. In the study region, the mineral assemblage of calcite + clinopyroxene + garnet + ferro-actinolite can be attributed to this facies.

Albite epidote-hornfels facies: This facie is the lowest temperature of contact metamorphic facies. Index minerals of this facie in the region include calcite, quartz, garnet, ferro-actinolite, and chlorite.

Table 2. The results of electron microprobe analysis of garnet in skarn of Dezg

	1 abie 2	. The resu	its of electi	con microp	TODE allaly	SIS OI gai II	et iii skai ii	of Dezg		
	grt	6153-	6153-	6153-	6153-	6153-	6153-	6153-	6153-	6153-
	Standard	grt1	grt2	grt3	grt5	grt6	grt7	grt8	grt9	grt10
SiO2	37.85	36.64	37.39	37.10	36.16	36.46	36.35	37.09	37.02	36.27
TiO2	0.01	0.60	0.36	0.16	0.57	0.72	0.36	0.79	0.88	1.37
Al203	21.60	5.22	8.30	8.45	5.38	6.58	4.94	7.16	7.63	6.06
Cr203	0.00	0.01	0.000	0.00	0.01	0.00	0.00	0.02	0.02	0.01
Fe0	32.52	25.17	19.73	19.45	24.89	22.19	24.88	21.43	20.47	23.87
MnO	1.10	0.85	0.20	0.21	0.78	0.48	0.61	0.22	0.18	0.32
MgO	6.02	0.11	0.03	0.03	0.12	0.15	0.07	0.16	0.17	0.15
CaO	0.79	32.47	35.09	34.73	32.39	33.67	33.24	33.44	34.12	33.02
Total	99.89	101.08	101.11	100.14	100.31	100.25	100.45	101.30	100.52	101.01
Formula(Corr.)	12(0)	12(0)	12(0)	12(0)	12(0)	12(0)	12(0)	12(0)	12(0)	12(0)
Si	2.990	2.932	2.940	2.942	2.913	2.916	2.923	2.927	2.939	2.896
Ti	0.001	0.036	0.021	0.010	0.035	0.043	0.022	0.047	0.052	0.082
Al	2.011	0.492	0.769	0.790	0.511	0.620	0.468	0.666	0.714	0.570
Cr	0.000	0.001	0.00	0.00	0.001	0.00	0.00	0.001	0.001	0.001
Fe+3	0.007	1.571	1.308	1.307	1.591	1.460	1.642	1.385	1.302	1.474
Fe+2	2.141	0.113	-0.011	-0.017	-0.066	-0.024	-0.031	-0.029	-0.057	0.114
Mn	0.074	0.057	0.013	0.014	0.053	0.032	0.041	0.014	0.012	0.022
Mg	0.709	0.013	0.003	0.004	0.014	0.018	0.008	0.018	0.020	0.017
Ca	0.067	2.784	2.956	2.951	2.789	2.886	2.864	2.912	2.902	2.824
XFe2(Vlll)	0.716	0.038	-0.004	-0.006	0.029	0.008	0.011	0.010	0.019	0.038
XMn(Vlll)	0.025	0.019	0.004	0.005	0.018	0.011	0.014	0.005	0.004	0.007
XMg(Vlll)	0.237	0.004	0.001	0.001	0.005	0.006	0.003	0.008	0.007	0.006
XCa(VIII)	0.022	0.938	0.948	1.000	0.948	0.975	0.973	0.979	0.0970	0.949
XAl(Vl)	0.996	0.239	0.370	0.377	0.243	0.298	0.222	0.325	0.354	0.279
XFe3(Vl)	0.004	0.761	0.630	0.623	0.757	0.702	0.778	0.675	0.648	0.721
XCr(Vl)	0.000	0.000	0.000	0.000	0.000	0.000	0.000	0.000	0.001	0.000
End-members										
Almandine	71.6	3.8	-0.4	-0.8	2.9	0.8	1.1	1.0	1.9	3.8
Spessartine	2.5	1.9	0.4	0.5	1.8	1.1	1.4	0.5	0.4	0.7
Pyrope	23.7	0.4	0.1	0.1	0.5	0.6	0.3	0.8	0.7	0.6
Grossular	2.2	22.4	37.0	37.7	23.0	29.1	21.6	31.8	34.3	26.4
Andradite	0.0	71.4	62.9	62.3	71.8	68.4	57.7	66.1	62.6	68.4
Uvarovite	0.0	0.0	0.0	0.0	0.0	0.0	0.0	0.0	0.1	0.0



Table 3. The results of electron microprobe analysis of pyroxene in skarns of Dezg

	6152	6152	6152	6152	6152	6152	6152	6152	6152	6152	6152	6152
Column 1	px1	6152 px2	6152 px3	6152 px4	6152 px5	px6	6152 px7	6152 px8	6152 px9	6152 px10	6152 px11	6152 px12
SiO2	55.67	53.24	52.09	52.42	52.74	51.34	52.77	52.44	52.24	52.40	51.30	52.45
TiO2	0.00	0.71	0.36	0.25	0.21	0.46	0.21	0.94	0.08	0.01	0.42	0.00
Al203	10.45	1.548	3.00	2.69	1.11	3.12	2.15	0.68	1.22	1.25	3.40	0.19
Cr203	0.00	0.00	0.25	0.63	0.07	0.02	0.78	0.02	0.04	0.00	0.35	0.17
FeO	5.05	6.55	6.36	5.08	8.73	7.35	4.52	9.45	10.00	12.43	6.03	12.37
MnO	0.00	0.00	0.19	0.12	0.16	0.12	0.12	0.29	0.32	0.38	0.14	0.44
MgO	8.26	14.06	15.30	16.31	13.56	13.23	16.69	11.97	11.91	10.76	15.81	11.13
CaO	11.18	23.98	22.74	22.31	23.80	24.42	222.98	24.33	24.34	23.62	21.52	24.16
Na20	7.70	0.344	0.47	0.21	0.61	0.56	0.18	0.30	0.25	0.35	0.19	0.22
K20	0.00	0.00	0.08	0.00	0.00	0.00	0.02	0.01	0.04	0.01	0.00	0.00
Total	96.33	100.094	100.83	100.01	100.99	100.62	100.41	100.43	100.45	101.22	99.56	101.42
Total	70.55	100.074	100.03	100.01	100.77	100.02	100.41	100.43	100.43	101.22	77.30	101.72
Fomula	6(0)	6(0)	6(0)	6(0)	6(0)	6(0)	6(0)	6(0)	6(0)	6(0)	6(0)	6(0)
Si	2.051	1.970	1.912	1.924	1.958	1.906	1.929	1.968	1.955	1.972	1.899	1.977
Ti	0.000	0.002	0.010	0.007	0.006	0.013	0.006	0.027	0.002	0.000	0.012	0.000
Al	0.454	0.072	0.130	0.116	0.049	0.137	0.093	0.030	0.054	0.056	0.0148	0.008
Cr	0.000	0.000	0.007	0.018	0.002	0.001	0.022	0.001	0.001	0.000	0.0140	0.000
Fe3+	0.000	0.000	0.000	0.000	0.000	0.000	0.000	0.000	0.000	0.000	0.000	0.000
Fe2+	0.154	0.203	0.195	0.156	0.271	0.228	0.138	0.297	0.314	0.391	0.187	0.390
Mn	0.000	0.006	0.006	0.004	0.005	0.004	0.003	0.009	0.010	0.012	0.004	0.014
Mg	0.344	0.776	0.837	0.892	0.751	0.732	0.909	0.570	0.668	0.604	0.873	0.626
Ca	0.442	0.951	0.894	0.877	0.947	0.972	0.900	0.978	0.981	0.952	0.870	0.994
Na	0.550	0.025	0.033	0.015	0.044	0.040	0.013	0.022	0.019	0.026	0.014	0.016
K	0.000	0.000	0.004	0.000	0.000	0.000	0.001	0.000	0.002	0.000	0.000	0.000
Total	3.997	4.004	4.028	4.009	4.033	4.032	4.015	4.001	0.016	4.013	4.017	4.026
Tri plots	0.777	1.001	1.020	1.007	1.000	1.002	1.010	1.001	0.010	1.010	11017	1.020
En	0.365	0.402	0.435	0.463	0.381	0.379	0.467	0.344	0.340	0.310	0.452	0.311
Fs	0.165	0.105	0.101	0.081	0.138	0.118	0.071	0.153	0.160	0.201	0.097	0.194
Wo	0.469	0.493	0.464	0.458	0.481	0.503	0.462	0.503	0.500	0.489	0.451	0.495
Jd	0.550	0.025	0.031	0.013	0.043	0.040	0.010	0.021	0.019	0.026	0.013	0.015
Ac	0.000	0.000	0.002	0.002	0.002	0.000	0.003	/0.000	0.000	0.000	0.001	0.001
Aug	0.450	0.975	0.957	0.985	0.965	0.960	0.987	0.978	0.981	0.974	0.986	0.984
	0.100	0.57.0	0.707	0.700	0.700	0.700	0.507	0.570	0.701	0.57.1	0.700	0.701
A(+aqw)	-0.054	0.012	0.026	0.030	0.002	0.024	0.026	0.002	0.009	0.008	0.036	-0.002
C(+aqw)	0.494	0.485	0.451	0.441	0.479	0.490	0.450	0.500	0.493	0.482	0.434	0.492
(FM)(+aqw)	0.559	0.503	0.523	0.529	0.519	0.586	0.525	0.498	0.498	0.510	0.530	0.510
Mole												
fractions												
XSi(T)	1.000	1.000	1.000	1.000	1.000	1.000	1.000	1.000	1.000	1.000	1.000	1.000
XAl(T)	0.000	0.000	0.000	0.000	0.000	0.000	0.000	0.000	0.000	0.000	0.000	0.000
XAl(M1)	0.454	0.072	0.130	0.116	0.049	0.137	0.093	0.030	0.054	0.056	0.148	0.000
XFe3(M1)	0.000	0.000	0.000	0.000	0.000	0.000	0.000	0.000	0.000	0.000	0.000	0.008
XFe2(M1)	0.154	0.197	0.177	0.139	0.260	0.223	0.125	0.296	0.310	0.378	0.163	0.384
XMg(M1)	0.340	0.753	0.759	0.793	0.720	0.717	0.822	0.669	0.658	0.683	0.763	0.616
XFe2(M2)	0.002	0.006	0.018	0.017	0.011	0.005	0.013	0.000	0.005	0.013	0.023	0.006
XMg(M2)	0.004	0.023	0.078	0.100	0.030	0.016	0.087	0.000	0.010	0.021	0.109	0.010
XCa(M2)	0.442	0.951	0.894	0.877	0.947	0.972	0.900	0.978	0.981	0.952	0.870	0.994
XNa(M2)	0.550	0.025	0.033	0.015	0.044	0.040	0.013	0.022	0.019	0.026	0.014	0.016
	0.000	0.020	0.000	0.010	0.011	0.010	0.010	<u> </u>	0.027	0.020	0.011	0.010

Table 4. The results obtained from calculation of temperature in the software on pyroxenes available in skarns (Kerog, 1988; Sengupta et al., 1989; Soto, 1993)

0 G F											
	S 1	S 2	S 3	S 4	S 5	S 6	S 7	S 8	S 9	S10	S 11
Raheim and Gree (1974)	477.8	435.8	643.33	2175.83	1011.23	1054.27	1172.8	1241.98	118.83	763.81	906.568
Kerog (1988)	327.93	308.98	494.11	3178.99	906.32	953.07	1105.89	1209.6	123.55	S10	921.68
Sengupta et al. (1989)	221.08	208.98	315.44	885.06	487.95	502.93	545.76	578.83	87.24	763.81	419.564
r Fe	3.304	3.535	3.923	4.5	9.107	4.187	4.35	4.258	0.775	S10	4.2245
r Mg	1.71	1.057	1.025	1.007	1.018	1.016	1.013	1.014	3.041	763.81	1.2276



Table 5. The results obtained from the calculation of pressure in the software by the garnet-pyroxene-plagioclase method in skarn (Powell and Holland, 1988; Eckert, 1991; Graham and Powell, 1984 et al., 1985)

garnet-pyroxene- plagioclase	C 1	C2	С3	C4	C5	C6	C7	C8	С9	C10
	S1	S2	S3	S4	S5	S6	S7	S8	S9	Average
Perkins and Newton (1981)	6.4	1.54	2.75	3.71	22	2.58	8.61	3.42	6.4	3.90125
Powell and Holland (1988)	8.71	1.9	3.19	4.21	2.55	2.98	9.39	12.199	0.1	4.564875
Esckert et al. (1991)	9.22	3.52	4.79	6	4.5	4.67	11.57	5.69	1.91	5.33125

Table 6. The results obtained from the calculation of temperature in the software by garnet-amphibole method

Column 1	Column 2
Garnet-amphibole	T(°c)
Graham & Powell (1984)	883.72
Perchuk et al. (1985)	385.37

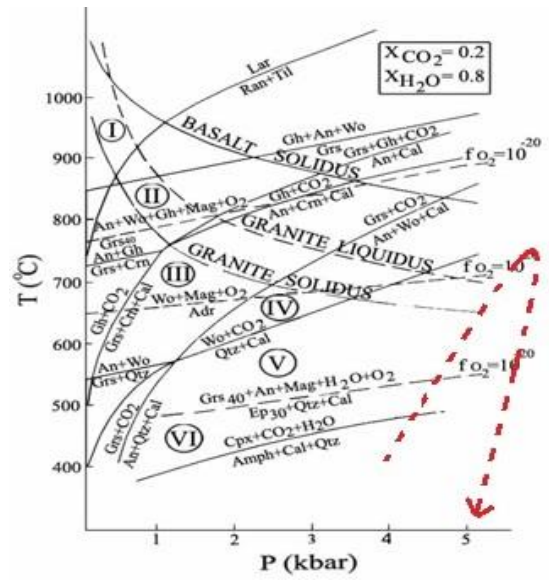


Fig. 8. The range of the facies in the skarn, in diagram P-T (Esmaeili, 2014)

VI. CONCLUSIONS

The results of the present study are as follows:

- According to the data of microprobe analysis, the garnets available in the skarn are andradite-grossular and have been formed at the expense of clinopyroxene.
- The composition skarn clinopyroxenes are diopside to augite diopside and hedenbergite.
- According to the results of the analyses, all clinopyroxenes have metamorphic nature, which indicates that this mineral has crystallized in metamorphic conditions.
- Two types of alteration in skarn system include primary prograde stage which is associated with anhydrous minerals like garnet and pyroxene, and final retrograde stage which is characterized by hydrous minerals including epidote, hornblende, calcite, quartz, and chlorite.
- Formation of anhydrous calcium silicate minerals like andradite, grossular, and clinopyroxene proves the

temperature range between 756 and $776^{\circ}C$ and XCO2=0.1-0.6.

- In retrograde metamorphism at temperatures lower than 756°C , an assemblage of anhydrous calcium silicate minerals has changed into hydrous silicate minerals like epidote minerals. Moreover, the assemblage of hydrous and anhydrous calcium silicate minerals undergo metamorphism and turn into fine mineral assemblages like chlorite, calcite, quartz, and clay minerals.
- Based on the minerals and temperature-pressure calculations of the skarn under investigation, two facies of hornblende-hornfels and albite epidote-hornfels were identified in this rock assemblages, which have been from most important factors in formation of Skarn of study area.

ACKNOWLEDGEMENTS

Sincere thanks go to Prof. Michael Brocker and Mr. Timon who helped with electron microprobe analysis of the samples in University of Münster, Germany.

REFRERENCES

Alavi Naeeini, M. (1981). Shahrokht's Geology Map 1:250000. Publication of Geology and National Mineral Discoveries Organization, 8056 pages.

Alavi Naeeini, M. (1982). Ahangaran's Geology Map 1:100000. Publication of Geology and National Mineral Discoveries Organization, 8056 pages.

Angiboust, Samuel, et al. (2013). Insights on deep, accretionary subduction processes from the Sistan ophiolitic "mélange" (Eastern Iran). Lithos 156: 139-158.

Bröcker M, Fotoohi Rad Gh. Burgess R . Theunissen st . .Paderin I., Rodionov N., Salimi Z. (2013). New age constraints for the geodynamic evolution of the Sistan Suture Zone, eastern Iran. Lithos 170: 17-34.

Cartwright J.A., (1994). Episodic basin-wide hydrofracturing of overpressured early Cenozoic mudrock sequences in the north sea basin. Marine and Petroleum Geology, 11, 587-607.

Daya AA., Biabangard H., Boomeri M. (2024). Identification of anomalies using multivariate fractal modeling in the Maleksiahkuh region, SE Iran, Journal of Analytical and Numerical Methods in Mining Engineering 14 (39), 13-25.

Daya AA., Hosseini-Nasab M. (2017). Identification of Geochemical Anomalies Using Fractal Analysis in Janja Area, SE Iran, 8th International Conference on Advances in Engineering and Technology (AET-17) Sept. 6-7, Budapest (Hungary).

Daya MM., Nasab MH. (2019). Application and comparison of the cokriging and the fractal model for identifying geochemical anomalies in Janja area, SE Iran, International Journal of Mining and Mineral Engineering 10 (1), 1-26.

Eckert, J. O. Jr., Newton, R.C.& Kleppa, O.J. (1991). Heat of reaction and recalibration of garnet-pyroxene-plagioclase-quartz geobarometers in CMAS system by solution calorimetry of stoichiometric mineral mixes. Am. Mineral., V. 79, 148-160.

Esmaeili, Z. (2014). Petrology of metamorphic rocks in Dezg (southwest of Shahrokht) east of Iran. Unpublished Petrology M.Sc. Thesis. Geology Department, Sciences Faculty, Birjand University, 105 pages.



Fotoohi Rad, G. R., et al. (2005). Eclogites and blueschists of the Sistan Suture Zone, eastern Iran: A comparison of P-T histories from a subduction mélange. Lithos 84.1: 1-24.

Fotoohi Rad, G.R. (2004). Petrology and geochemistry of metamorphic ophiolites in east of Birjand. PhD Dissertation, Teacher Training University of Tehran, 323 pages.

Graham C. and Powell R. (1984). A garnet – hornbelende geothermometer :calibration, testing and application to the Pelona schist, southern California. Journal of Metamorphic Geology, , V. 2, Issue 1. P.13-31.

Jamteveit, B., Sevensen, H., Podladchikov, W., Planke, S. (1992). Hydrothermal vent complexes associated with sill intrusions in sedimentary basins. Vent complexes in sedimentary basins ,233-241.

Kerog, E.J. (1988). The garnet – clinopyroxene Fe-Mg geothermometer – a reinterpretation of existing experimental data. Contributions to Mineralogy and Petrology. 99: 44-48.

Kretz, R., (1994). Metamorphic Crystallization. Chichester, New York, Brisbane, Toronto, Singapore:, John Wiley & Sons.

Meinert, L. (2013). Skarn deposits – Characteristics and Exploration Criteria. Mineral Resources Program, USGS December 3-5, GEUS Tungsten Assessment Workshop.

Mercier, J.C.C. (1980). Single –pyroxene thermometry. Tectonophysics, 70:1-37.

Parkins D. and Newton R.C. (1981). Charnockite geobarometers based on coexisting garnet-pyroxene – plagioclase – quartz, Nature, , V. 292, P. 144-146.

Perchuk L.L., Aranovich L.Ya., poslesskil K., Lavrenteva I.V., Gerasimov V.Ya., Fedkin, V.V., Kitsul V.I., Karsakov L.P. and Berdnikov N.V. (1985). Precamberian granulites of the aldan shield, eastern Siberia, USSR. Journal of Metamorphic Geology, , V. 3, Issue 3, P.265-310.

Powell, R. and Holland, T.J.B. (1988). An internally consistent thermodynamic dataset with uncertainties and corellations: 3 applications to geobarometry, worked examples and a computer program. Journal of Metamorphic Geology.

Råheim, A., & Green, D.H. (1974). Experimental petrology of lunar highland basalt composition and applications to models for the lunar interior. The Journal of Geology, 82(5), 607-622.

Sengupta P., Dasgupta S, Bhatacharya P.K. and Haria Y. (1989). Mixing behavior in quaternary garnet solid solution and an extended Ellis and Green garnet-clinopyroxene geothermometer. Contribution to Mineralogy and Petrology, , V. 103, Issue 2, P. 223-227.

Soto J.I. and Soto V.M. (1993). PTMAFIC: Software package for thermometry, barometry, and activity calculations in mafic rocks using an IBM-compatible computer. Computers & Geosciences, C21(5):619-652

Tirrul R., Bell L.R., Griffis R.J. and Camp V.E. (1983); , The Sistan suture zone of eastern Iran: G.S.A. Bulletin , $v.\,84$, $p.\,134-140$.

Yardley B.W.D. (1981). Effect of cooling on the water content and mechanical behavior of metamorphosed rocks. Geology, V. 9, p. 405-408

Zhai, D., Liu, J., Wang, J., Yang, Y., Zhang, H., Wang, X., Zhang, Q., Wang, G. and Liu, Zh. (2014). Zircon U–Pb and molybdenite Re–Os geochronology, and whole-rock geochemistry of the Hashitu molybdenum deposit and host granitoids, Inner Mongolia, NE China. Journal of Asian Earth Sciences, V. 79, Part A., P. 144-160.

Zharikov V.A. (1991). Types of skarns, formation and ore mineralization. In, Skarns - their genesis and metallogeny. Theophrastus Publ. S.A., Athens, Greece. pp. 455-466.